Ligand and support effects on the reactivity and stability of $Au_{38}(SR)_{24}$ catalysts in oxidation reactions

Bei Zhang[1], Clara García[2], Annelies Sels[1], Giovanni Salassa[1], Christoph Rameshan[2], Jordi Llorca[3], Klaudia Hradil [4], Günther Rupprechter[2], Noelia Barrabés[2*] and Thomas Bürgi[1*]

[1] *Department of Physical Chemistry, University of Geneva, Quai Ernest-Ansermet 30, CH-1211 Geneva, Switzerland*

[2] *Institute of Materials Chemistry, Technische Universität Wien, Getreidemarkt 9/BC/01, 1060 Vienna, Austria*

[3] *Institute of Energy Technologies, Department of Chemical Engineering and Barcelona Research Center in Multiscale Science and Engineering, Universitat Politècnica de Catalunya, EEBE, Eduard Maristany 16, 08019 Barcelona,Spain*

[4] *X-Ray Center, TU Wien, Getreidemarkt 9, 1060 Vienna, Austria*

Corresponding authors:

Noelia Barrabés (noelia.rabanal@tuwien.ac.at)

Thomas Bürgi (Thomas.buergi@unige.ch)

Abstract

Thiolate protected metal nanoclusters are emerging materials for the preparation of atomically defined heterogeneous catalysts. Recently it was revealed that the ligands migrated to the support upon cluster deposition, which influences the catalytic behaviour. Here we examined the role of the protecting thiolate ligands on the cyclohexane oxidation for $Au_{38}(SR)_{24}$ supported on CeO_2 and Al_2O_3. Sulfur containing products were detected. XANES S K-edge measurements revealed SO_x species on the support during the reaction. The results indicate (i) an active and complex role of the thiolate ligand and (ii) changes of cluster (surface) structure, depending on support material and reaction conditions.

Graphical Abstract

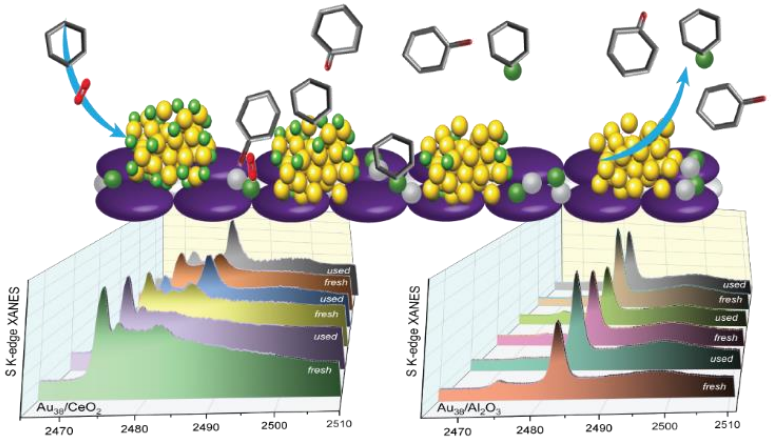

Keywords: gold; nanoclusters, thiolate ligands, heterogeneous catalysis; oxidation reaction; xafs, surface

Highlights

- Unexpected product distribution is related to thiol-surface interaction.
- SO_x species evolution during reaction depends on the support material.
- Cluster structure stability differences observed with both support materials.

Introduction

Thiolate protected Au nanoclusters in the size range from sub-nanometer to 2 nm have shown extraordinary catalytic selectivity and activity, which are dependent on both their size and structure [1, 2]. To enhance stability and activity of the catalyst, Au nanoclusters are supported on various materials for heterogeneous catalytic oxidation reactions such as CO oxidation [3, 4], cyclohexane oxidation [2, 5] aerobic alcohol oxidation [6] or styrene oxidation [7]. Au nanoclusters are atomically precise and composed of a dense gold core and protecting S-(Au-S)$_n$- (n= 1, 2) units (staples) [8]. The atomic level homogeneity and the well-defined surface of Au nanoclusters make them a promising model catalyst to study the structure-reactivity correlation at atomic level [9].

In addition to the influence of the support material [5, 10] the thiolate ligands play an important role in the catalytic activity of Au nanoclusters in some reactions depending on the level of ligand coverage around the Au cluster core (with ligands partially removed by thermal treatments) [11-13]. Supported ligand protected clusters ($Au_x(SR)_y/CeO_2$, x=25, 38 and 144), were active in reactions such as CO oxidation, although the discussion of the ligands effect was controversial. Whereas in some works higher activity were obtained without removing any ligands [14, 15], in another case it was reported that the thiol ligands act as a double-edged sword. In this case, the ligands stabilize the Au cluster structure, but block CO adsorption on Au sites [4]. Therefore, partial removal of thiolate ligands was typically required for CO oxidation. In the case of liquid phase aerobic oxidation of benzyl alcohol, $Au_{25}(SC_{12}H_{25})_{18}$ supported on porous carbon nanosheets showed no activity with the completed ligand shell, but only when the ligands were partly removed. The ligand coverage also affects selectivity since thiolates reduce the oxidation ability of Au by withdrawing electrons, but also by inducing site isolation [6].

Our previous work demonstrated that the catalytic activity and selectivity of Au_{38}/M_xO_y (M_xO_y= Al_2O_3 and CeO_2) can be fine-tuned via the thiolate coverage and the type of support material, modulating the nanocluster-support interaction [5]. Liquid phase aerobic cyclohexane oxidation was the target reaction studied. Au (III) complex and nanoscale Au catalysts supported on metal oxides [16] and carbon materials[17] have been applied in this reaction leading to high selectivity towards cyclohexanone and cyclohexanol at low conversion level. Cyclohexane oxidation reactions occur at the nanoparticle-support interface of the supported Au nanoparticles catalysts, where Au nanoparticles promote the activation of O_2 molecules and accelerate the formation of surface active oxygen species [18]. Tsukuda *et al*. studied the cluster size effect on the cyclohexane oxidation reaction, showing that Au_{39} exhibits highest catalytic activity among various Au_n nanoclusters (n= 10, 18, 25, 39, 85) [2].

Based on this, in our previous work, supported $Au_{38}(SR)_{24}$ cluster catalysts were studied in the reaction evaluating the effect of the pretreatment and of the support material [5]. Clear differences in the catalytic activity were obtained depending on the degree of the thiolate ligand removal. Surprisingly, unexpected cyclohexanethiol was observed among the products, being a clear evidence of the active role of the thiolate ligands in the reaction. The only possible source of sulfur to form cyclohexanethiol is the thiolate ligand (SR), proving their direct participation in the reaction.

In our recent study, we revealed for the first time ligand migration from the gold cluster to the support[19]. We studied the fate of the thiolate ligands upon supporting $Au_{38}(SC_2H_4Ph)_{24}$ nanoclusters on oxides surfaces and the evolution under oxidative pretreatments. S K-edge XAFS (X-ray Absorption Spectroscopy) disclosed the formation of unexpected oxidized sulfur species on the support [19]. The redistribution and oxidation of the ligands modified the support surface, a factor that may alter its properties.

Herein we explore the active role of thiolate protecting ligands in a catalytic reaction, studying the interaction between the gold clusters and the oxide support of the used catalysts (Au_{38}/M_xO_y (M_xO_y= Al_2O_3 and CeO_2)) in the cyclohexane oxidation [5] by spectroscopic techniques. Electronic properties of S species have been investigated by X-ray absorption near edge structure (XANES). Evolution of the catalysts surface was followed by XAFS, UV-vis spectroscopy, high-angle annular dark-field scanning transmission electron microscopy (STEM-HAADF), X-ray photoelectron spectroscopy (XPS) and *in situ* attenuated total reflection infrared spectroscopy (ATR-IR), revealing different size growth depending on the oxide support material and ….

Experimental

Catalysts preparation and cyclohexane oxidation reaction

Synthesis and characterization as well as the catalytic activity of Au_{38}/M_xO_y catalysts were described in detail previously [5]. Shortly, $Au_{38}(SC_2H_4Ph)_{24}$ was synthesized and separated by size exclusion chromatography (SEC). $Au_{38}(SC_2H_4Ph)_{24}$ is denoted as Au_{38} in the following. The monodispersity of Au nanocluster was confirmed by MALDI-TOF mass spectrometry. The obtained $Au_{38}(SC_2H_4Ph)_{24}$ was then supported on Al_2O_3 and CeO_2 (at 0.5 wt % Au) by impregnation. A solution of the Au_{38} cluster in dichloromethane (DCM) and the oxide materials was stirred until the brown solution turned colourless. Supported clusters samples are denoted as Au_{38}Al and Au_{38}Ce, respectively. The supported nanocluster catalysts were collected by filtration and dried in air at 80˚C.

Thermal pretreatments of the supported nanoclusters were carried out in air at 150 °C and 250 °C (10°C/min ramp). Each catalyst was tested in the aerobic cyclohexane oxidation reaction using reported method [5], with the reaction mixtures being analysed by gas chromatography coupled with mass spectrometry (GC-MS).

Characterization techniques

UV-vis spectra of the solid samples were recorded on a UV/VIS spectrometer (Perkin Elmer 750 Lambda) coupled with a Diffuse Reflectance Sphere. Samples were placed in quartz cuvettes and $BaSO_4$ was used as reference.

High-angle annular dark field (HAADF)-Scanning Transmission Electron Microscopy (STEM) was performed at 200 kV with a Tecnai G2 F20 S-TWIN microscope equipped with a field emission electron source and provided the microstructural characterization.

X-ray photoelectron spectroscopy (XPS) measurements were performed on a UHV system equipped with a Phoibos 100 hemispherical analyzer and a XR 50 X-ray source (SPECS GmbH). Spectra were recorded with AlKα radiation and data were analyzed with the CasaXPS software. Peaks were fitted after Shirley (Au-signal) and Linear (S-signal) background subtraction with Gauss−Lorentz sum functions. Peak positions and full width at half-maximum (FWHM) were left unconstrained. Au 4f peaks were fitted with 3.7 eV doublet separation and a fixed ratio of 4:3 for $Au4f_{7/2}$ an $Au4f_{5/2}$. For the S 2p peak fitting doublets with a fixed doublet separation of 1.2 eV and a fixed area ratio of 2:1 were used for $S2p_{3/2}$ and $S2p_{1/2}$ (all NIST XPS database). For the XPS measurements the powders were applied evenly on carbon tape. Peak positions were referenced to the C1s (graphite) and valence band signal.

Attenuated Total Reflection (ATR) infrared spectroscopy was performed with a Vertex 70 (Bruker Optics) spectrometer equipped with a liquid-nitrogen-cooled mercury cadmium telluride (MCT) detector and a commercial mirror unit (SN 854). The ZnSe crystal was drop casted with an ethanol suspension of the sample and let dry, creating a thin catalysts. The experiments were performed with a Spec commercial flow cell connected in recycling configuration (batch) with the vessel containing the reaction mixture (cyclohexane, oxygen bubbler and initiator) The system was heated to 60 °C (temperature closest to the catalytic measurements, but avoiding evaporation). A series of consecutive spectra (200 scans per spectrum; resolution 4 cm^{-1}) was collected (20 s/spectra) for 2 hours.

XAFS studies

X-ray absorption fine structure (XAFS) measurements at the S K-edge (2.4720 keV) and Au L_3-edge (11.9187 keV) were carried out at the BL22-CLAESS beamline at the ALBA

synchrotron (Barcelona, Spain) for both the fresh, thermal pretreated and used catalysts. The samples were prepared as 5 mm pellets and mounted on the beamline sample holder. Measurements at both S K-edge and Au L_3-edge were performed in fluorescence mode under vacuum and low temperature conditions (liquid nitrogen T≈ 80K). Sulfur reference compounds (sulfur, sulfone, Na_2SO_3, Na_2SO_4, corresponding oxidation states: 0, +3, +4, and +6; and Al_2O_3 and CeO_2 supported phenylethanethiol) were also measured. Additional XAFS measurements at Au L_3-edge for selected CeO_2 supported catalysts were carried out at the Super-XAS beamline at the Swiss Light Source (Villigen, Switzerland). Fluorescence signal was detected with five-element SDD detector (SGX). The powder samples were placed in a quartz capillary and cooled down with a cryo-gun to liquid nitrogen temperature. The data analysis was performed according to standard procedures using Ifeffit software [20].

Results and Discussion

Ligand effect

The catalytic activity of Au_{38} clusters supported on CeO_2 and Al_2O_3 was studied for the aerobic oxidation of cyclohexane in our previous work [5]. Surprisingly, a significant amount of cyclohexanethiol was found, revealing the active participation of the sulfur species in the catalytic reaction (Figure S1). This is more pronounced in the case of Al_2O_3 support. In both cases, cyclohexanol production increases upon rising the pretreatment temperature, which could be due to more catalytically active Au atoms exposed upon heating and some increase in the particle size. Cyclohexanethiol was obtained in both cases but in higher amount in the case of $Au_{38}Al$ catalysts. It has been proposed that the formation of cyclohexanethiol is directly related with residual ligands of the Au_{38} cluster on the support, which is the only source of S atoms in the supported nanocluster catalysts [5]. The Evolution of the unexpected product (cyclohexanethiol) was study with longer reaction times. Figure 1b shows the decrease in the cyclohexanethiol presents in the products mixture, gradually in the case of $Au_{38}Ce$ in comparison to the $Au_{38}Al$ catalysts with a sharp decay. It is accompanied with an increase in the selectivity to the desired products, more pronounced in the case of ketone formation.

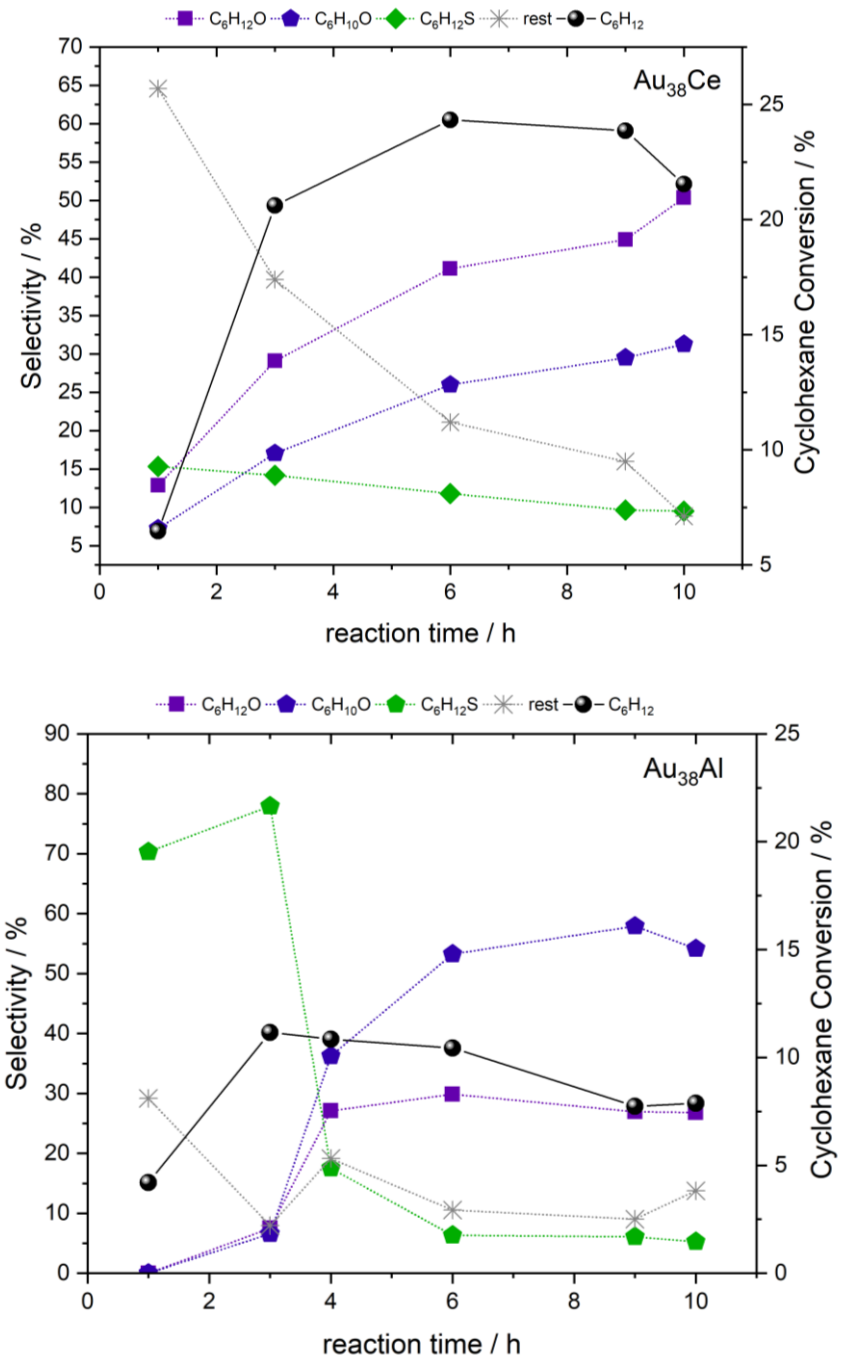

Figure 1. Catalytic activity of Au_{38}/MO_x (CeO_2 and Al_2O_3) in the cyclohexane oxidation reaction

Interaction of sulfur compounds with oxides such as Al_2O_3 and CeO_2 have been studied for desulfurization or absorption of thiols [21-23]. The reactivity for the adsorption and dissociation of S-containing molecules on oxides depends on their properties such as acidity-basicity properties, pore structure, band gaps, presence and type of oxygen vacancies, etc. The treatment of these oxides with sulfur dioxide can lead to the formation of sulfite species, which is more effective in case of CeO_2 related with a higher Lewis basicity strength in comparison with alumina. In these cases, chemisorbed sulfite on alumina decreased at the

same time that physisorbed SO_2 increased [21]. CeO_2 supported Au nanoparticles oxidize a wide variety of aromatic and heterocyclic thiols to disulfides even at room temperature, using oxygen as electron acceptor. This catalyst applies for both aqueous and solvent-free conditions [22]. This could explain different interactions between the thiolate ligands and different support materials, which dictate their catalytic behaviour.

In order to get more insights into these interactions, in situ ATR experiments were performed with $Au_{38}Ce$ and $Au_{38}Al$ catalysts, as well as with each support fresh and with thiolate ligand impregnated (SRCe and SRAl) during cyclohexane oxidation. Like in previous studies [10], the reactivity can be observed with the evolution of the characteristic cyclohexane vibrations (Figure S2), in the ν(C-H) range. Around 2929 and 2849 cm^{-1}, symmetric and asymmetric stretching vibrations of the cyclohexane CH_2 groups are detected, respectively. Cyclohexane scissoring, twisting and rocking characteristic vibrations were observed in lower wavenumber region (1447 and 1014 cm^{-1}), as well as bending modes (1258 cm^{-1}) [24].These samples are not leading to high activity in the cyclohexane oxidation , which, is evidenced by the absence of characteristic bands of the main products cyclohexanone or cyclohexanol in the spectra. Only in the case of gold supported catalysts, a shoulder around 1467cm^{-1} related to cyclohexanol formation is observed.

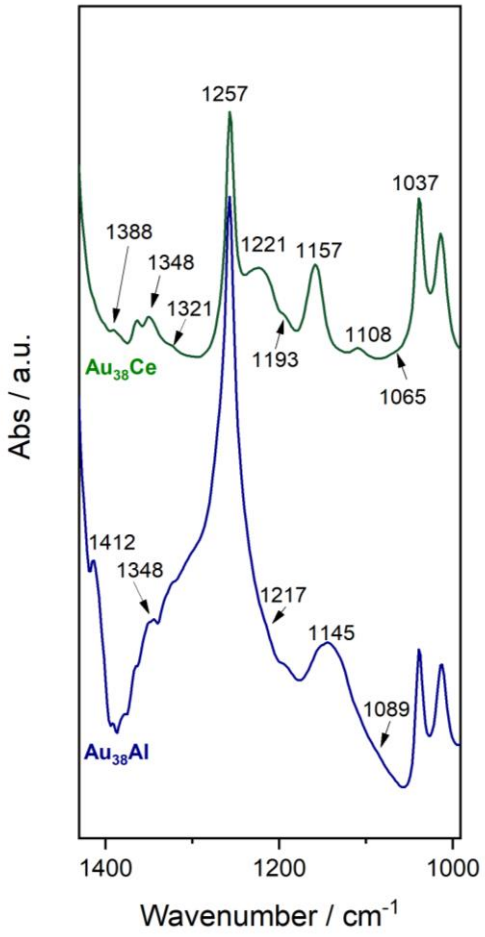

Figure 2. ATR spectra of $Au_{38}Ce$ and $Au_{38}Al$ after 1 hours during the in situ cyclohexane oxidation reaction

The interaction of the ligands with the support leading to SO_x species can be demostrated by S=O and S-O vibrations. Previous reported studies assigned bands around 1340, 1373, 1145 and 1050 cm^{-1} to the adsorbed SO_x species on oxides materials like Al_2O_3 [25-28]. In figure 2 the three bands at 1055, 1145 and 1362 cm^{-1}(marked in red) can be assigned to SO_x species. This shows the formation of sulphur oxide species on the catalysts surface, in agreement with the XAFS measurements. Then, this species can be the source for the formation of cyclohexanethiol, which have the infrared characteristic bands around 1340, 1220, 1190, 1030 and 1019 cm^{-1}. In figure 2 are detected the bands at 1348, 1217, 1221 and 1193 cm^{-1} with both catalysts during the reaction that can be assigned to this unexpected product in agreement with in the kinetic measurements

In addition, the interaction of the S species and formation of oxides upon deposition and their evolution under pretreatment was confirmed and proved in our recent work.[29] In order to explain the observed selectivity during the cyclohexane oxidation from our previous study,[5] which are likely related with the thiolate ligand coverage and interaction with the support, the evolution of the S species was followed by XAFS measurements at the S K-edge.

With thiolate protected gold cluster samples, EXAFS measurements are limited due to contribution from Au M_3-edge (2.7430 keV) which is very close to S K-edge (2.4720 keV). The signal from Au M_3-edge would therefore overlap with the post-edge oscillations, which limits the k-space (EXAFS region) spectrum until 8 $Å^{-1}$. However, the XANES region is enough to determine the formal oxidation state of the element, because the absorption edge energy changes related to the oxidation state of the absorbing atom. Identification of the S species in the collected samples was carried out by comparing the experimental XANES spectra with S reference compounds (oxidation states: -1, 0, +3, +4 and +6). Unsupported Au_{38} clusters showed a pre-edge feature at 2471 eV related to S-Au bond and a S-C peak at 2473 eV, in agreement with previously reported measurements [29-31]. When supported on metal oxides, the S-Au peak intensity decreases as compared to the S-C peak intensity. New peaks corresponding to S species at high oxidation states (disulfide, SO_3^{-2} and SO_4^{-2}) were also observed (Figure S3).

Both atmospheric and support lattice oxygen may contribute to the formation of high oxidation state S species from detached thiolate ligands. For both metal oxides supported nanocluster samples different oxidation states of S were observed. In $Au_{38}Al$, S-O peaks at

2482 and 2497 eV are related with SO_3^{-2} and SO_4^{-2}, which formed by the reaction between support lattice oxygen and SO_2 [32]. In $Au_{38}Ce$, S-O peaks at 2478 and 2481 eV are related to SO_3^{-2}.The different oxidation states of S species in the supported nanocluster catalysts are therefore attributed to different interactions between the support and the S species. This is further confirmed by the fact that the oxides supported phenylethanethiol reference samples show similar peaks to their Au_{38}/M_xO_y counterpart (Figure S3).

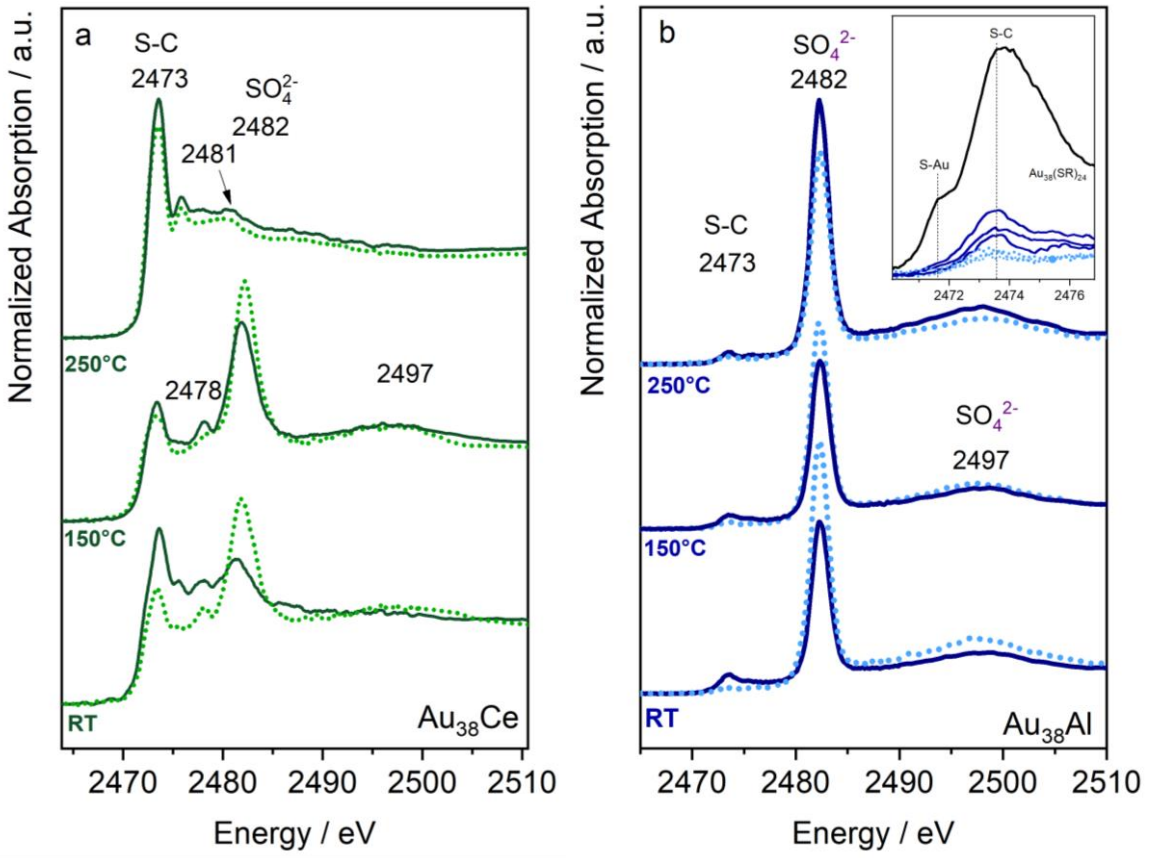

Figure 3. XANES spectra at S K-edge of Au_{38}/MO_x catalysts without pretreatment (RT) and after pretreatment, before reaction (—) and after cyclohexane oxidation reaction (●●●): a: CeO_2 and b: Al_2O_3 supported catalysts.

During the aerobic oxidation of cyclohexane, the S-C peak decreases, denoting the ligand removal or fragmentation of the carbon chain part, with a simultaneous increase of the S-O peak in $Au_{38}Ce$ mainly with the fresh and 150°C pre-treated sample, as is shown in Figure 3. This could be explained by the participation of low oxidation state sulfur species in the reaction or the further oxidation of the S species under O_2 rich reaction conditions. The same trend is observed for $Au_{38}Al$ samples. In the case of thermally pre-treated samples at 250°C, S-O peak decreases during the reaction. Possibly this is due to higher reactivity when more gold surface is available due to higher pretreatment temperatures.

The redistribution of S species in the supported samples affects the oxidation reaction possibly in two ways: *1)* Direct participation of the S species adsorbed on the support in the reaction; *2)* Poisoning of the catalytic active site on the support surface and affecting the charge transfer between support and nanocluster. Firstly, the rich library of S species in the support sample offers the starting material for the formation of cyclohexanethiol. Secondly, the adsorption of sulfur species (either on metal sites or oxygen vacancies) changes the charge distribution on the surface, which is related with the activation of the O_2 molecule and charge transfer between the support and the nanocluster. Jin and coworkers reported an enhanced catalytic activity of $Au_{38}Ce$ catalyst in CO oxidation by increasing the Ce^{3+}/Ce^{4+} ratio in the support [33]. This finding gives important insight into the effect of nanocluster pre-treatment and reaction conditions.

Cluster stability under cyclohexane oxidation reaction

The Au L_3-edge XANES spectra probe transitions of 2p to unoccupied 5d states of the Au atoms in the clusters, therefore the Au-thiolate bonding in these structures can be studied. The white line intensity increases from bulk to cluster structure, indicating a d-electron depletion as size decreases. From calculations, it was concluded that the staple (non-metallic) Au site shows more pronounced d-electron depletion than the (metallic) core Au site [30, 34]. In the case of $Au_{38}Ce$ catalysts, only the sample without pretreatment was possible to be measured after reaction due to the low amount of recovered sample and the challenging measurement in fluorescence mode, due to the strong signal from the CeO_2 support. Figure S4a shows the XANES spectra of $Au_{38}Ce$: before and after cyclohexane oxidation, presenting slight changes in the white line and peaks at 11920eV and 11950eV related with the decrease in Au-S bonds and increase in the fraction of Au-Au bonds. No further relevant structural changes are observed in this case (peak at 11970eV). However, in the case of $Au_{38}Al$ catalysts, XANES spectra before and after pretreatment; and after reaction could be obtained (Figure S4b). By increasing the temperature of the pretreatment, a higher tendency to the metallic state, decreasing and shifting the white line (≈11920eV) is observed. Pronounced changes in the peak around 11950eV are visible with increasing temperature. This can be related to a decrease of Au-S bonds during pretreatment, resulting in an increase in the fraction of the Au-Au bonds, leading to higher metallic character. This can also be related, together with changes in the peak around 11970eV, to an increase of cluster size, loss of the cluster structure and formation of more bulk structure, in line with the decrease of the white line. This shows that sintering of the clusters supported on Al_2O_3 occurs already during the pretreatment and more pronounced during the reaction.

STEM-HAADF studies were performed to investigate the size and morphology of the samples before and after reaction. Figure 4 shows $Au_{38}Al$ and $Au_{38}Ce$ catalysts fresh, pretreated at 250°C, and after cyclohexane oxidation reactions. Upon supporting on Al_2O_3 and CeO_2, Au nanoclusters (bright dots in the images) exhibit homogeneous size distribution with a diameter around 1nm.

In the case of $Au_{38}Ce$ catalysts (Fig.4, green line), the ceria support is constituted by small nanoparticles of about 4-7nm in size. They do not exhibit any particular shape. Concerning Au, it is very difficult to identify the Au clusters but, when visible, they measure about 1nm or they are even subnanometric. There is an excellent distribution of Au clusters. The sample after reaction is virtually identical to the fresh one without any Au cluster sintering evidenced. This is also the case for the sample pretreated at 250°C shown in Figure 4 that looks identical to the fresh one. It is important to highlight that most of the Au clusters are still subnanometric or about 1nm, and only a few clusters measuring about 1.5nm are present.

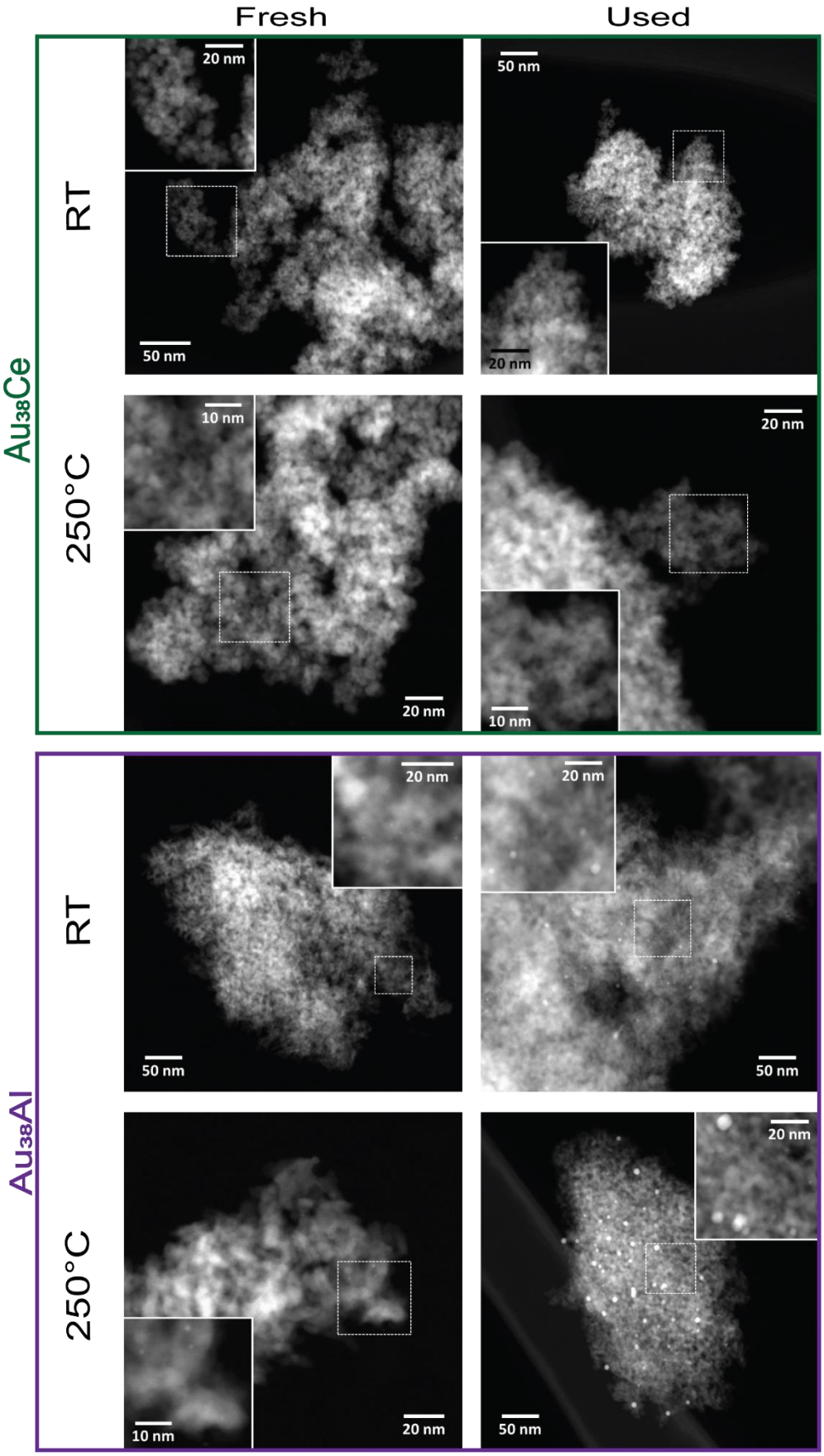

Figure 4. HAADF-STEM images from before (fresh) and after cyclohexane oxidation reaction (used) of Au_{38}/M_xO_y (CeO_2 and Al_2O_3), without pretreatment and after pretreatment at 250°C.

In the case of $Au_{38}Al$ catalysts (Fig.4, lila line), the fresh sample without pretreatment, presents bright dots corresponding to Au clusters, which are very homogeneous in size and measure about 1 nm in diameter. After 24h of reaction the sample mainly exhibits Au clusters of about 1nm, but there are a few Au clusters measuring 1.5-2nm, suggesting a slight sintering. For $Au_{38}Al$ pretreated at 250°C, it is observed that some of the Au clusters sinter into Au nanoparticles with a rather broad size distribution. Some of the initial Au clusters persist, which are identified by their size of about 1 nm, but larger Au nanoparticles are clearly visible, mostly in the size range of 2-3 nm, while some of them measure up to 4 nm. Most pronounced sintering is observed in this sample after reaction where the Au clusters have agglomerated strongly into Au nanoparticles in the range 2-10 nm in diameter. The distribution of Au nanoparticle size is quite heterogeneous.

The UV spectra of supported Au_{38} have been studied and compared (Figure S5). Three main peaks (480, 626, and 750nm) are observed for the unsupported Au_{38}. Discrete transitions and molecular-like electronic properties of $Au_{38}(SR)_{24}$ have been identified by density-functional theory computations, which suggests that the ligand HOMO → LUMO transitions contribute partially to the experimentally observed peaks at 626nm and 750nm [35].

The Au_{38} features (480, 626 and 750nm) in Au_{38}/Al_2O_3 decrease with treatment temperature (Figure S5) and no feature of Au_{38} is observed after treatment at 250˚C, denoting a loss in the cluster structure which can be related to the ligand removal. After reaction, only obvious plasmonic band at the wavelength range of 530-540nm is detected in the recovered $Au_{38}Al$ sample (Figure S3), which reveals the size growth of nanocluster. Higher intensity of plasmonic peak in each used sample (with and without thermal pretreatment) is observed after longer reaction time. In the case of $Au_{38}Ce$, the well defined features associated to the Au_{38} clusters are hardly visible after the pretreatment. Not obvious plasmonic peak is present in the UV-vis spectra neither after the pretreatment or the reaction. Comparing to $Au_{38}Al_3$, $Au_{38}Ce$ the absence of plasmonic peak shows that CeO_2 stabilizes the Au core during reaction in agreement with the HAADF-STEM measurements. These findings can be related to different support-S species and support-Au cluster interaction in $Au_{38}Al$ and $Au_{38}Ce$ samples. Higher stability of the cluster structure is obtained with CeO_2 compared to Al_2O_3, in agreement with previous works [5].

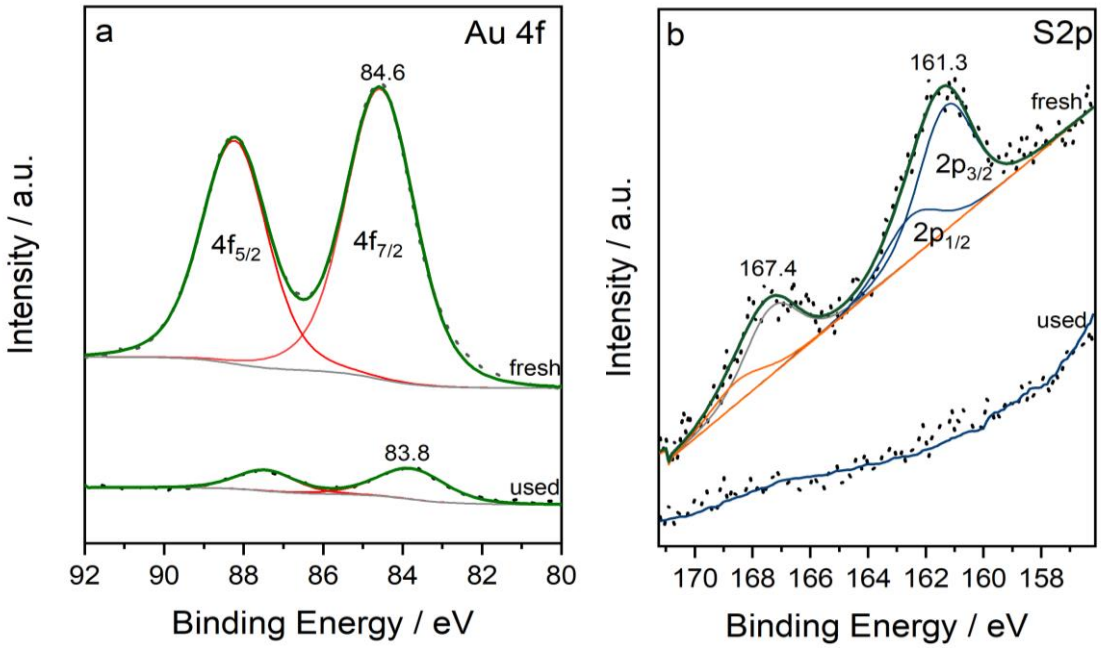

Figure 5. XPS spectra of (a) the Au 4f and (b) the S 2p3 core levels of the Au_{38} clusters supported on ceria. Bottom spectra are acquired after cyclohexane oxidation reaction (used) and before (fresh)

XPS analysis was performed before and after catalytic reaction to characterize the gold clusters and to determine the state of sulfur in CeO_2 supported catalyst. Figure 4 shows the respective Au 4f and S 2p regions, including peak fitting. After pretreatment, a Au4f7/2 signal can be observed at 84.6 eV and can be attributed to metallic gold. The binding energy is ~ 0.6 eV higher than for bulk metallic Au. Huang et al. reported similar binding energies for Au-nanoclusters supported on ceria [36]. Furthermore, the peak position is in line with earlier work on monolayer protected Au-clusters[19]. Also, Zhang showed for AuSR nanoparticles of decreasing size, that the Au 4f peaks shift to higher binding energy [37]. This shift results from a nanosize effect and from metal−ligand interactions in the surface of nanoparticles and clusters.[37] After reaction, the Au4f signal changed significantly, showing a strong shift to lower binding energies (83.8 eV). This could be due to strong metal-support interaction. Similar low binding energies were reported by Si et al. for Au supported on ceria nanocubes (used for water gas shift reaction) [38].

In the S 2p spectra (Figure 4b), the spectrum of the fresh $Au_{38}Ce$- sample after pretreatment at 150°C comprises two components at 161.3 and 167.4 eV. The peak at 161.3 eV can be attributed to the sulfur-gold bond, in agreement with values for metal sulphides or with the Au-S bond in self assembled monolayers. The peak at 167.4 eV can be assigned to fully oxidized sulfur. This agrees with the results of Devillers et al. who reported oxidation of sulfur for self-assembled monolayers in an oxygen environment [39]. The XPS results for the oxidized sulfur correspond well to the observation of SO_3^{-2} and SO_4^{-2} in the XANES

measurements. After catalytic reaction no sulfur species were observed by XPS. This goes in line with the formation of cyclohexanethiol during reaction (i.e the sulfur is reacting with cyclohexane) and its disappearance in longer reaction times.

Conclusions

The active role of protecting thiolate ligands in Au_{38}/M_xO_y (Al_2O_3 and CeO_2) samples has been identified by detecting sulfur species on the support (originating from thermal treatment of catalysts) and in samples recovered after aerobic cyclohexane oxidation reaction. The migration of the thiol ligands to the support surface upon deposition of the gold nanoclusters created oxidized sulfur species that further evolved during the reaction. A different redistribution was observed depending on the nature of the oxide support. Therefore, the active sites on the support and the charge transfer between support and nanocluster are affected, which influences the catalytic properties. The unexpected formation of cyclohexanethiol in our previous studies was clarified, showing that the S species on the support surface (detached from the clusters), were available to react with the cyclohexane reactant. The cyclohexanethiol presence decrease over longer times leading to higher ketones mainly production. The continuous evolution of S species and dependence on the support material influence the reaction pathways and explain the complex selectivity previously observed for different oxidation reactions.

Upon S redistribution, the stability of the gold core also depends on the metal oxide. The CeO_2 support was shown to be better than Al_2O_3 in preventing gold nanocluster aggregation upon thermal treatment and during reaction. This study highlights the important role thiolate ligands play in supported Au nanocluster model catalysts.

Acknowledgments

T.B. acknowledges the financial support by the Swiss National Science Foundation grant number 200020_152596 and by the University of Geneva. G.R. received support by the Austrian Science Fund (FWF) (grants DK+ Solids4Fun W1243; SFB FOXSI F4502). J.L. is a Serra Húnter Fellow and is grateful to the ICREA Academia Program and grants MINECO/FEDER ENE2015-63969-R and GC 2017 SGR 128. B.Z. acknowledges a Chinese Scholarship Council Fellowship (201300120634). CG and NB thank the TUW Innovative Project GIP165CDGC.ALBA and SLS synchrotrons are acknowledged for beamtime at the CLAESS beamline (Proposal ID: 2015091489 and 2016091918) and at the SuperXAFS beamline (Proposal ID: 20161366).

References

[1] G. Li, D.E. Jiang, S. Kumar, Y.X. Chen, R.C. Jin, Size Dependence of Atomically Precise Gold Nanoclusters in Chemoselective Hydrogenation and Active Site Structure, Acs Catalysis, 4 (2014) 2463-2469.10.1021/cs500533h

[2] Y.M. Liu, H. Tsunoyama, T. Akita, S.H. Xie, T. Tsukuda, Aerobic Oxidation of Cyclohexane Catalyzed by Size-Controlled Au Clusters on Hydroxyapatite: Size Effect in the Sub-2 nm Regime, Acs Catalysis, 1 (2011) 2-6.Doi 10.1021/Cs100043j

[3] J. Good, P.N. Duchesne, P. Zhang, W. Koshut, M. Zhou, R. Jin, On the functional role of the cerium oxide support in the Au38(SR)24/CeO2 catalyst for CO oxidation, Catalysis Today, 280 (2017) 239-245.https://doi.org/10.1016/j.cattod.2016.04.016

[4] Z. Wu, D.-e. Jiang, A.K.P. Mann, D.R. Mullins, Z.-A. Qiao, L.F. Allard, C. Zeng, R. Jin, S.H. Overbury, Thiolate Ligands as a Double-Edged Sword for CO Oxidation on CeO2 Supported Au25(SCH2CH2Ph)18 Nanoclusters, Journal of the American Chemical Society, 136 (2014) 6111-6122.10.1021/ja5018706

[5] B. Zhang, S. Kaziz, H. Li, M.G. Hevia, D. Wodka, C. Mazet, T. Burgi, N. Barrabes, Modulation of Active Sites in Supported Au-38(SC2H4Ph)(24) Cluster Catalysts: Effect of Atmosphere and Support Material, Journal of Physical Chemistry C, 119 (2015) 11193-11199.10.1021/jp512022v

[6] T. Yoskamtorn, S. Yamazoe, R. Takahata, J.-i. Nishigaki, A. Thivasasith, J. Limtrakul, T. Tsukuda, Thiolate-Mediated Selectivity Control in Aerobic Alcohol Oxidation by Porous Carbon-Supported Au25Clusters, ACS Catalysis, 4 (2014) 3696-3700.10.1021/cs501010x

[7] M. Turner, V.B. Golovko, O.P.H. Vaughan, P. Abdulkin, A. Berenguer-Murcia, M.S. Tikhov, B.F.G. Johnson, R.M. Lambert, Selective oxidation with dioxygen by gold nanoparticle catalysts derived from 55-atom clusters, Nature, 454 (2008) 981-U931.10.1038/nature07194

[8] R.C. Jin, C.J. Zeng, M. Zhou, Y.X. Chen, Atomically Precise Colloidal Metal Nanoclusters and Nanoparticles: Fundamentals and Opportunities, Chemical Reviews, 116 (2016) 10346-10413.10.1021/acs.chemrev.5b00703

[9] J. Zhao, R. Jin, Heterogeneous catalysis by gold and gold-based bimetal nanoclusters, Nano Today, 18 (2018) 86-102.https://doi.org/10.1016/j.nantod.2017.12.009

[10] C. García, S. Pollitt, M. van der Linden, V. Truttmann, C. Rameshan, R. Rameshan, E. Pittenauer, G. Allmaier, P. Kregsamer, M. Stöger-Pollach, N. Barrabés, G. Rupprechter, Support effect on the reactivity and stability of Au25(SR)18 and Au144(SR)60 nanoclusters in liquid phase cyclohexane oxidation, Catalysis Today, (2018).https://doi.org/10.1016/j.cattod.2018.12.013

[11] R.R. Nasaruddin, T. Chen, N. Yan, J. Xie, Roles of thiolate ligands in the synthesis, properties and catalytic application of gold nanoclusters, Coordination Chemistry Reviews, 368 (2018) 60-79.https://doi.org/10.1016/j.ccr.2018.04.016

[12] Y. Li, Y. Chen, S.D. House, S. Zhao, Z. Wahab, J.C. Yang, R. Jin, Interface Engineering of Gold Nanoclusters for CO Oxidation Catalysis, ACS Applied Materials & Interfaces, 10 (2018) 29425-29434.10.1021/acsami.8b07552

[13] X.-K. Wan, J.-Q. Wang, Z.-A. Nan, Q.-M. Wang, Ligand effects in catalysis by atomically precise gold nanoclusters, Science Advances, 3 (2017).10.1126/sciadv.1701823

[14] W.L. Li, Q.J. Ge, X.G. Ma, Y.X. Chen, M.Z. Zhu, H.Y. Xu, R.C. Jin, Mild activation of CeO2-supported gold nanoclusters and insight into the catalytic behavior in CO oxidation, Nanoscale, 8 (2016) 2378-2385.10.1039/c5nr07498c

[15] X.T. Nie, C.J. Zeng, X.G. Ma, H.F. Qian, Q.J. Ge, H.Y. Xu, R.C. Jin, CeO2-supported Au-38(SR)(24) nanocluster catalysts for CO oxidation: a comparison of ligand-on and -off catalysts, Nanoscale, 5 (2013) 5912-5918.10.1039/c3nr00970j

[16] L.-X. Xu, C.-H. He, M.-Q. Zhu, S. Fang, A highly active Au/Al2O3 catalyst for cyclohexane oxidation using molecular oxygen, Catalysis Letters, 114 (2007) 202-205.10.1007/s10562-007-9058-0

[17] S.A.C. Carabineiro, L.M.D.R.S. Martins, M. Avalos-Borja, J.G. Buijnsters, A.J.L. Pombeiro, J.L. Figueiredo, Gold nanoparticles supported on carbon materials for cyclohexane oxidation with hydrogen peroxide, Appl Catal a-Gen, 467 (2013) 279-290.10.1016/j.apcata.2013.07.035

[18] P. Wu, P. Bai, Z. Yan, G.X.S. Zhao, Gold nanoparticles supported on mesoporous silica: origin of high activity and role of Au NPs in selective oxidation of cyclohexane, Scientific Reports, 6 (2016) 18817.10.1038/srep18817

[19] B. Zhang, A. Sels, G. Salassa, S. Pollitt, V. Truttmann, C. Rameshan, J. Llorca, W. Olszewski, G. Rupprechter, T. Bürgi, N. Barrabés, Ligand Migration from Cluster to Support: A Crucial Factor for Catalysis by Thiolate-protected Gold Clusters, ChemCatChem, 10 (2018) 5372-5376.doi:10.1002/cctc.201801474

[20] B. Ravel, M. Newville, ATHENA, ARTEMIS, HEPHAESTUS: data analysis for X-ray absorption spectroscopy using IFEFFIT, J. Synchrotron Radiat., 12 (2005) 537-541.doi:10.1107/S0909049505012719
[21] M.Y. Smirnov, A.V. Kalinkin, A.V. Pashis, A.M. Sorokin, A.S. Noskov, K.C. Kharas, V.I. Bukhtiyarov, Interaction of Al2O3 and CeO2 Surfaces with SO2 and SO2 + O2 Studied by X-ray Photoelectron Spectroscopy, The Journal of Physical Chemistry B, 109 (2005) 11712-11719.10.1021/jp0508249
[22] A. Corma, T. Rodenas, M.J. Sabater, Aerobic oxidation of thiols to disulfides by heterogeneous gold catalysts, Chemical Science, 3 (2012) 398-404.10.1039/C1SC00466B
[23] J.A. Rodriguez, J. Hrbek, Interaction of sulfur with well-defined metal and oxide surfaces: Unraveling the mysteries behind catalyst poisoning and desulfurization, Accounts of Chemical Research, 32 (1999) 719-728.Doi 10.1021/Ar9801191
[24] A.R. Almeida, J.A. Moulijn, G. Mul, In Situ ATR-FTIR Study on the Selective Photo-oxidation of Cyclohexane over Anatase TiO2, The Journal of Physical Chemistry C, 112 (2008) 1552-1561.10.1021/jp077143t
[25] M. Waqif, O. Saur, J.c. Lavalley, S. Perathoner, G. Centi, Nature and mechanism of formation of sulfate species on copper/alumina sorbent-catalysts for sulfur dioxide removal, The Journal of Physical Chemistry, 95 (1991) 4051-4058.10.1021/j100163a031
[26] Z. Wu, C. Li, Z. Wei, P. Ying, Q. Xin, FT-IR Spectroscopic Studies of Thiophene Adsorption and Reactions on Mo2N/γ-Al2O3 Catalysts, The Journal of Physical Chemistry B, 106 (2002) 979-987.10.1021/jp011577l
[27] F. Ouyang, R.-s. Zhu, K. Sato, M. Haneda, H. Hamada, Promotion of surface SOx on the selective catalytic reduction of NO by hydrocarbons over Ag/Al2O3, Appl. Surf. Sci., 252 (2006) 6390-6393.https://doi.org/10.1016/j.apsusc.2006.01.052
[28] M.B. Mitchell, V.N. Sheinker, M.G. White, Adsorption and Reaction of Sulfur Dioxide on Alumina and Sodium-Impregnated Alumina, The Journal of Physical Chemistry, 100 (1996) 7550-7557.10.1021/jp9519225
[29] B. Zhang, A. Sels, G. Salassa, S. Pollitt, V. Truttmann, C. Rameshan, J. Llorca, W. Olszewski, G. Rupprechter, T. Bürgi, N. Barrabes, Ligand migration from cluster to support: A crucial factor for catalysis by thiolate-protected gold clusters, ChemCatChem, 0 (2018).doi:10.1002/cctc.201801474
[30] D.M. Chevrier, R. Yang, A. Chatt, P. Zhang, Bonding properties of thiolate-protected gold nanoclusters and structural analogs from X-ray absorption spectroscopy, Nanotechnol Rev, 4 (2015) 193-206.10.1515/ntrev-2015-0007
[31] D. Stellwagen, A. Weber, G.L. Bovenkamp, R. Jin, J.H. Bitter, C.S.S.R. Kumar, Ligand control in thiol stabilized Au38 clusters, RSC Advances, 2 (2012) 2276-2283.10.1039/C2RA00747A
[32] J.A. Rodriguez, T. Jirsak, A. Freitag, J.C. Hanson, J.Z. Larese, S. Chaturvedi, Interaction of SO2 with CeO2 and Cu/CeO2 catalysts: photoemission, XANES and TPD studies, Catalysis Letters, 62 (1999) 113-119.Doi 10.1023/A:1019007308054
[33] J. Good, P.N. Duchesne, P. Zhang, W. Koshut, M. Zhou, R.C. Jin, On the functional role of the cerium oxide support in the Au-38(SR)(24)/CeO2 catalyst for CO oxidation, Catalysis Today, 280 (2017) 239-245.10.1016/j.cattod.2016.04.016
[34] P. Zhang, X-ray Spectroscopy of Gold-Thiolate Nanoclusters, Journal of Physical Chemistry C, 118 (2014) 25291-25299.10.1021/jp507739u
[35] Y. Pei, Y. Gao, X.C. Zeng, Structural prediction of thiolate-protected Au-38: A face-fused bi-icosahedral Au core, Journal of the American Chemical Society, 130 (2008) 7830-+.10.1021/ja802975b
[36] X.S. Huang, H. Sun, L.C. Wang, Y.M. Liu, K.N. Fan, Y. Cao, Morphology effects of nanoscale ceria on the activity of Au/CeO2 catalysts for low-temperature CO oxidation, Applied Catalysis B-Environmental, 90 (2009) 224-232.10.1016/j.apcatb.2009.03.015
[37] P. Zhang, X-ray Spectroscopy of Gold–Thiolate Nanoclusters, The Journal of Physical Chemistry C, 118 (2014) 25291-25299.10.1021/jp507739u
[38] R. Si, M. Flytzani-Stephanopoulos, Shape and crystal-plane effects of nanoscale ceria on the activity of Au-CeO2 catalysts for the water-gas shift reaction, Angewandte Chemie-International Edition, 47 (2008) 2884-2887.10.1002/anie.200705828
[39] S. Devillers, A. Hennart, J. Delhalle, Z. Mekhalif, 1-Dodecanethiol Self-Assembled Monolayers on Cobalt, Langmuir, 27 (2011) 14849-14860.10.1021/la2026957